Proceedings of the Eighteenth International Conference on
Civil, Structural and Environmental Engineering Computing
Edited by: P. Iványi, J. Kruis and B.H.V. Topping
Civil-Comp Conferences, Volume 10, Paper 10.4
Civil-Comp Press, Edinburgh, United Kingdom, 2025
ISSN: 2753-3239, doi: 10.4203/ccc.10.10.4

Towards a Consistent Co-Rotational Formulation for 3D Solid Finite Elements: Mathematical Comparison of Crisfield's and Felippa's Formulation

R. Páleník[1,2] and Z. Poruba[2]

[1] IT4Innovations, VSB – Technical University of Ostrava, Czech Republic
[2] Department of Applied Mechanics, Faculty of Mechanical Engineering, VSB – Technical University of Ostrava, Czech Republic

Abstract

The co-rotational formulation offers a fast and numerically stable pseudo-linear approach for solving structural problems involving large displacements and small strains. In this study, two well-established co-rotational formulations, Crisfield's and Felippa's, are rewritten using a unified notation to enable a direct comparison for 3D solid finite elements. Felippa's consistent formulation targets beams and shells, while Crisfield's approach includes 3D solids but is not fully consistent. Despite different initial appearances, the deformational displacement vectors and internal force vectors are shown to be mathematically identical, guaranteeing the same displacement response. However, the tangent stiffness matrices differ: Crisfield's omits complex terms, resulting in slower convergence, whereas Felippa's consistent version is expected to require fewer Newton–Raphson (NR) iterations. Additionally, this study presents easy-to-implement matrix forms of Crisfield's matrix A and Felippa's spin-fitter matrix G, for 3D solid

elements with a rotation matrix obtained via polar decomposition. This work lays the foundation for a forthcoming paper on a new consistent co-rotational formulation for 3D solid elements in a simple matrix form for efficient nonlinear analysis.

Keywords: co-rotational formulation, finite element method, solid finite elements, geometrically nonlinear analysis, consistent tangent stiffness matrix, polar decomposition, spin-fitter matrix

1 Introduction

The co-rotational (CR) formulation is a widely used technique for solving geometrically non-linear (NL), small-strain structural problems in a pseudo-linear manner. In this approach, a local coordinate system (LCS) is rigidly attached to each finite element so that it undergoes the same translation and rotation. This allows the element's rigid body motion to be separated from its total displacements based on the position of the LCS relative to the inertial global coordinate system (GCS). The remaining deformational displacements, responsible for strain, are assumed to be small and are therefore handled using the linear small-strain theory within the element. As such, CR formulation can be regarded as a filter of rigid body motion.

The concept of the CR technique in the finite element method (FEM) was introduced in the early 1970s by Wempner [1] and Belytschko [2]. A significant advancement came with the element-independent co-rotational (EICR) procedure proposed by Rankin and Brogan [3], which has since become a standard. A key advantage of the EICR is that it operates on the precomputed linear element stiffness matrix without modifying Gauss-based element kernels. This allows for the reuse of linear elements, including any enhancements, in geometrically NL analyses.

Over the past four decades, the EICR approach has been successfully extended from beam and shell finite elements (FEs) to 2D and eventually 3D solid FEs, driven by growing computational capabilities. The EICR formulation for 3D solid FEs was established by Crisfield and Moita [4, 5, 6]. Although their formulation is described as consistent, the tangent stiffness matrix is artificially symmetrized due to the neglect of higher-order terms arising in its derivation. This simplification has been widely adopted, as the resulting inconsistent tangent stiffness matrix still provides good convergence. However, a truly consistent tangent stiffness matrix ensures optimal convergence, as it corresponds to the Hessian of the strain energy and is therefore symmetric [7, 8]. The approach to compute the truly consistent tangent stiffness matrix was presented by Felippa and Haugen in [9, 10], though their work focused on beam and shell FEs.

The objective of this paper is to provide a clear and complete mathematical description of Crisfield's and Felippa's CR formulations, specifically for 3D solid FEs. Both approaches are reformulated using a unified notation, allowing for direct identification of similarities and differences. The formulations are expressed in a ready-to-implement matrix form, with emphasis on the interpretation of the mathematical expressions used.

This work extends the earlier conference paper [11], which compares NL and CR algorithms for static analysis and demonstrates the numerical advantages of the CR one. In this paper, all computations are performed per element. While EICR formulations can incorporate material nonlinearity, a linear-elastic material model is used in the element kernel for simplicity.

2 Crisfield's co-rotational formulation

The Crisfield's CR formulation for solid finite elements was established by Crisfield and Moita and is well explained in [6].

2.1 Rotation matrix

The origin of the LCS can be arbitrarily determined because rigid body translation does not influence internal force computation. Crisfield and Moita have chosen node 1 of the element as the origin of the LCS. The rotation matrix is computed via the polar decomposition of the deformation gradient computed at the element centroid.

By definition, polar decomposition $\boldsymbol{F} = \boldsymbol{R}\boldsymbol{U}$ is a mathematical tool that decomposes a square matrix $\boldsymbol{F}$, representing the deformation gradient, onto an orthogonal matrix $\boldsymbol{R}$, representing the rotation matrix, and a symmetric matrix $\boldsymbol{U}$, representing the right stretch tensor.

The mathematical expression for the rotation matrix can be derived as follows.

$$\boldsymbol{F}^\top \boldsymbol{F} = (\boldsymbol{R}\boldsymbol{U})^\top (\boldsymbol{R}\boldsymbol{U}) = \boldsymbol{U}^\top \boldsymbol{R}^\top \boldsymbol{R}\boldsymbol{U} = \boldsymbol{U}^\top \boldsymbol{U} = \boldsymbol{U}\boldsymbol{U}, \tag{1}$$

where the relations $\boldsymbol{R}^{-1} = \boldsymbol{R}^\top$ and $\boldsymbol{U} = \boldsymbol{U}^\top$ were used. From the derivation of Eq. (1), the relation for the stretch tensor follows as

$$\boldsymbol{U} = (\boldsymbol{F}^\top \boldsymbol{F})^{\frac{1}{2}}, \tag{2}$$

and substituting Eq. (2) into the polar decomposition definition gives the relation for the rotation matrix

$$\boldsymbol{R} = \boldsymbol{F}\boldsymbol{U}^{-1} = \boldsymbol{F}(\boldsymbol{F}^\top \boldsymbol{F})^{-\frac{1}{2}}. \tag{3}$$

Such a computed rotation matrix exactly represents the rigid body rotation at the element centroid, and its computation is independent of element node ordering. However, the linear triangular FE in 2D and the linear tetrahedral FE in 3D are the only solid elements with constant deformation gradient. All the other FEs can have different deformation gradient and therefore also a different rigid body rotation at their various points, e.g., in nodes or Gauss points. Intuitively, if a single rotation matrix shall represent the rigid body rotation of the FE, the rotation matrix computed at the element centroid can be assumed to be the best possible approximation of the true mean rigid body rotation of the whole element.

Crisfield and Motia propose the polar decomposition of the deformation gradient computed in the element centroid for the rotation matrix computation because it enforces the zero local spin at the element centroid, which, as originally proposed in [12] for a 2D case, satisfies the large strain patch test.

In [6], the 3×1 local spin vector, which is set to zero, is defined as

$$\overline{\boldsymbol{\Omega}} = \boldsymbol{A}^\top \overline{\boldsymbol{u}} = \boldsymbol{0}, \tag{4}$$

where $\boldsymbol{A}$ is a $3N \times 3$ matrix which is computed from initial coordinates and is therefore constant during NR iterations. The computation of this unnamed matrix is partly shown in [13, 6], but only for 2D solid elements. To the knowledge of the authors of this paper, the computation of the $\boldsymbol{A}$ matrix, labeled as $\boldsymbol{B}_{\mathrm{S}}$ in [14], has never been published for 3D solid elements simply in a matrix form for the ease of implementation.

In 3D, the Eq. (4) takes the following form

$$\overline{\boldsymbol{\Omega}} = \begin{bmatrix} \frac{\partial \overline{w}_{\mathrm{o}}}{\partial y_0} - \frac{\partial \overline{v}_{\mathrm{o}}}{\partial z_0} \\ \frac{\partial \overline{u}_{\mathrm{o}}}{\partial z_0} - \frac{\partial \overline{w}_{\mathrm{o}}}{\partial x_0} \\ \frac{\partial \overline{v}_{\mathrm{o}}}{\partial x_0} - \frac{\partial \overline{u}_{\mathrm{o}}}{\partial y_0} \end{bmatrix} = \boldsymbol{A}^\top \overline{\boldsymbol{u}} = \begin{bmatrix} 0 \\ 0 \\ 0 \end{bmatrix}, \tag{5}$$

where each row represents a zero rotation with respect to the local axes *x*, *y* and *z*, and e.g. local displacement at the element centroid in the direction of the *x* axis is

$$\overline{u}_o = \sum_{i=1}^{N} h_{i,\mathrm{o}}\, \overline{u}_i, \tag{6}$$

where $h_{i,\mathrm{o}}$ is a shape function of the i-th node evaluated at the element centroid and $\overline{u}_i$, as part of the vector $\overline{\boldsymbol{u}}$, is a nodal displacement of the node i in the direction of the local *x* axis.

Then the $3N \times 3$ matrix $\boldsymbol{A}$ can be written in a matrix form as

$$\boldsymbol{A} = \begin{bmatrix} -\mathrm{spin}(\boldsymbol{B}_1) \\ \cdots \\ -\mathrm{spin}(\boldsymbol{B}_i) \\ \cdots \\ -\mathrm{spin}(\boldsymbol{B}_N) \end{bmatrix} = \begin{bmatrix} \mathrm{spin}(\boldsymbol{B}_1) & \cdots & \mathrm{spin}(\boldsymbol{B}_i) & \cdots & \mathrm{spin}(\boldsymbol{B}_N) \end{bmatrix}^\top, \tag{7}$$

where $\boldsymbol{B}_i$ is the i-the column of the following standard [1] $3 \times N$ matrix of shape functions derivatives with respect to initial coordinates

$$\boldsymbol{B} = \begin{bmatrix} \cdots & \frac{\partial h_{i,\mathrm{o}}}{\partial x_0} & \cdots \\ \cdots & \frac{\partial h_{i,\mathrm{o}}}{\partial y_0} & \cdots \\ \cdots & \frac{\partial h_{i,\mathrm{o}}}{\partial z_0} & \cdots \end{bmatrix} = \frac{\partial \boldsymbol{h}_{\mathrm{o}}}{\partial \boldsymbol{x}_0} = \boldsymbol{J}^{-\top} \frac{\partial \boldsymbol{h}_{\mathrm{o}}}{\partial \boldsymbol{\xi}} = \left(\frac{\partial \boldsymbol{h}_{\mathrm{o}}}{\partial \boldsymbol{\xi}} \boldsymbol{X}_0^\top \right)^{-1} \frac{\partial \boldsymbol{h}_{\mathrm{o}}}{\partial \boldsymbol{\xi}}, \tag{8}$$

where $\boldsymbol{x}_0 = [x_0, y_0, z_0]^\top$ is a vector of initial nodal coordinates, $\boldsymbol{X}_0$ is a $3 \times N$ matrix of initial nodal coordinates of all element nodes in the GCS, $\boldsymbol{h}_{\mathrm{o}}$ is a vector of N shape

[1] standardly reshaped into the $6 \times 3N$ matrix $\boldsymbol{B}$ and used for e.g. strain computation

functions evaluated at the element centroid after its derivative, $\boldsymbol{\xi} = [\xi, \eta, \zeta]^\top$ is a vector of natural coordinates, and $\boldsymbol{J}$ is a Jacobi matrix.

The operator *spin* is related to the cross-product, as defined e.g. in [6, 9, 7], and it transforms any 3×1 vector $\boldsymbol{r} = [r_1, r_2, r_3]^\top$ into the skew-symmetric matrix as follows

$$\text{spin}(\mathbf{r}) = \mathbf{r}\times = \begin{bmatrix} 0 & -r_3 & r_2 \\ r_3 & 0 & -r_1 \\ -r_2 & r_1 & 0 \end{bmatrix} = -\text{spin}(\mathbf{r})^\top. \tag{9}$$

There are more approaches to computing the rotation matrix form the deformation gradient. Some iterative methods, see e.g. [14], may be computationally faster than directly utilizing the Eq. (3), which requires computation of eigenvalues of a 3×3 matrix.

Knowing the $\boldsymbol{B}$ matrix, the deformation gradient can be efficiently computed as follows

$$\boldsymbol{F} = \boldsymbol{I} + \boldsymbol{D} = \boldsymbol{I} + \boldsymbol{U}\,\boldsymbol{B}^\top, \tag{10}$$

where $\boldsymbol{I}$ is a 3×3 identity matrix, $\boldsymbol{D}$ is the so called (global) displacement derivative matrix and $\boldsymbol{U}$ is a $3 \times N$ matrix of (global) nodal displacements of all N element nodes in x, y, z directions.

2.2 Local deformational displacements

The local deformational displacement vector of a general node i is in [6] expressed as

$$\overline{\boldsymbol{u}}_i = \boldsymbol{R}^\top(\boldsymbol{x}_i - \boldsymbol{x}_1) - (\boldsymbol{x}_{i,0} - \boldsymbol{x}_{1,0}) = \boldsymbol{R}^\top \boldsymbol{x}_{i\text{o}} - \boldsymbol{x}_{i\text{o},0}, \tag{11}$$

where $\boldsymbol{x}_i$ and $\boldsymbol{x}_1$ are the global coordinates of nodes i and 1, respectively, in the current, i.e., deformed configuration, and $\boldsymbol{x}_{i,0}$ and $\boldsymbol{x}_{1,0}$ are the global coordinates of nodes i and 1, respectively, in the initial configuration.

Figure 1 shows the computation of the local deformational displacement vector for a general node i, shown for simplicity in 2D. The term $\boldsymbol{x}_{i\text{o}} = \boldsymbol{x}_i - \boldsymbol{x}_1$ in Eq. (11) is a coordinate of the node i with respect to the LCS origin, here node 1, in the current configuration. This coordinate is then rotated back to the initial configuration orientation via the multiplication by $\boldsymbol{R}^\top$. Finally, the initial coordinate of the node i with respect to the initial LCS origin $\boldsymbol{x}_{i\text{o},0}$ is subtracted from it to obtain the local deformational displacement of the node i, which is assumed to be small.

In general, the $3N \times 1$ local deformational displacement vector of a finite element can be expressed as

$$\overline{\boldsymbol{u}} = \text{diag}(\boldsymbol{R}^\top)(\boldsymbol{u} + \boldsymbol{x}_0 - \boldsymbol{u}_\text{o} - \boldsymbol{x}_{\text{o},0}) - \overline{\boldsymbol{x}}_0, \tag{12}$$

where the operator *diag* forms a block diagonal matrix of N copies of the 3×3 rotation matrix $\boldsymbol{R}$, so that each rotation matrix corresponds to each node, $\boldsymbol{u}$ is a vector of the (global) nodal displacements, $\boldsymbol{x}_0$ is a vector of the initial nodal coordinates, $\boldsymbol{u}_\text{o}$ and

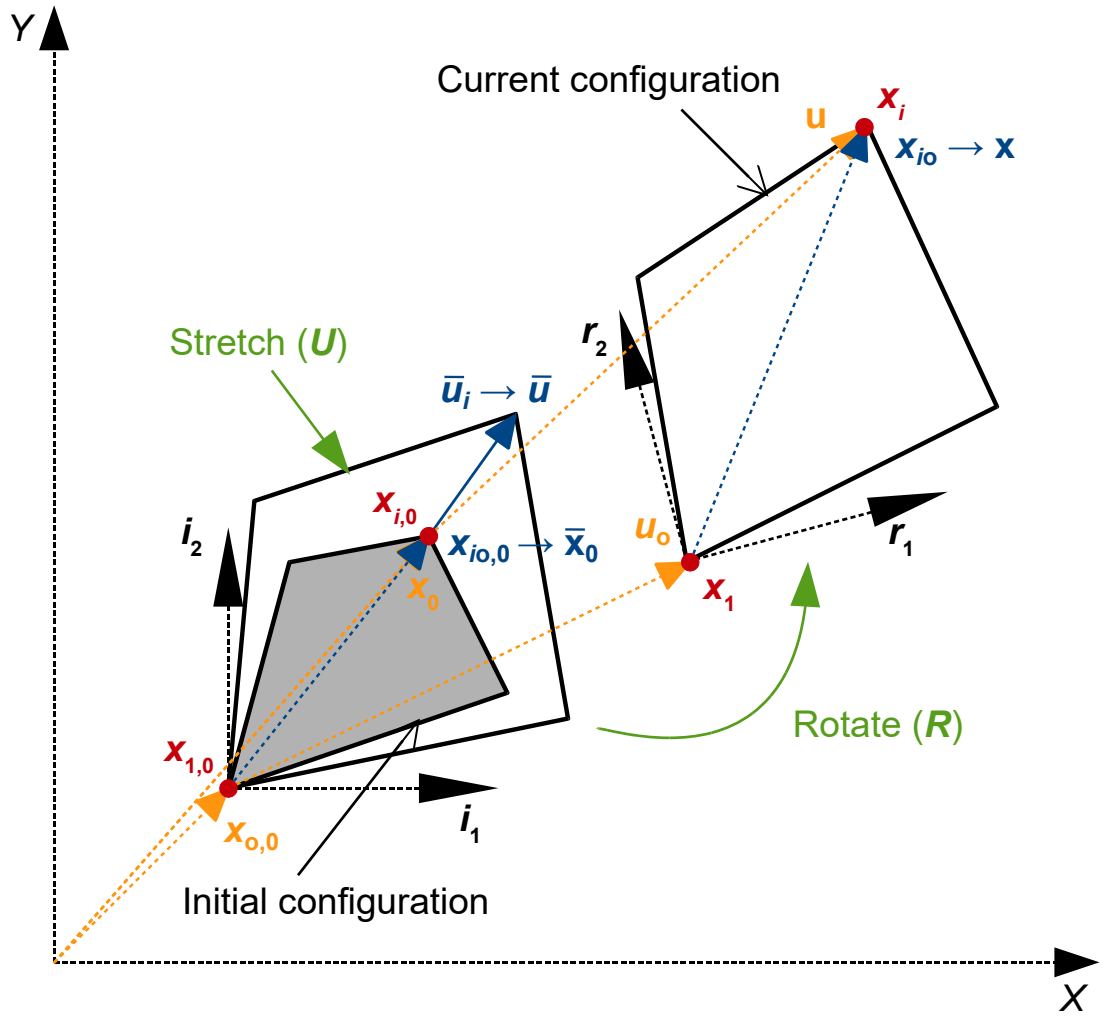

Figure 1: Kinematics of the CR solid finite element: computation of the local deformational displacement for a general node i (in red and blue) and as a vector for all element nodes (in orange and blue)

$\boldsymbol{x}_{\mathrm{o},0}$ are the vectors of N copies of the (global) displacements and initial coordinates of the LCS origin, [2] respectively, and $\overline{\boldsymbol{x}}_0 = \boldsymbol{x}_0 - \boldsymbol{x}_{\mathrm{o},0}$ is the vector of local [3] initial nodal coordinates.

The vectors $\boldsymbol{u}_\mathrm{o}$ and $\boldsymbol{x}_{\mathrm{o},0}$ represent the rigid body translations of the element. Although these vectors may be useful, for example, when plotting a meaningful magnitude of the deformational displacements, they can be excluded from Eq. (12) for the subsequent computation of the internal force vector. The rigid body displacements lie in the null space of the stiffness matrix and therefore cannot produce any deformational force. This is the reason why the origin of the LCS can be arbitrarily chosen.

Therefore, the local deformational displacement vector, which is further used, has

[2] The LCS origin can be chosen arbitrarily. Typically, it is a node 1 or element centroid.
[3] Local means with respect to the LCS.

the following simplified form

$$\overline{\boldsymbol{u}} \equiv \operatorname{diag}(\boldsymbol{R}^\top)\boldsymbol{x} - \overline{\boldsymbol{x}}_0, \tag{13}$$

where $\boldsymbol{x} = \boldsymbol{u} + \boldsymbol{x}_0$ is the nodal coordinate vector in the current configuration.

2.3 Internal force

The resistance to deformation of the small-strain element is given by the linear stiffness matrix $\overline{\boldsymbol{K}}$. The internal force vector

$$\boldsymbol{f} = \left(\frac{\partial \varphi}{\partial \boldsymbol{u}}\right)^\top = \left(\frac{\partial \varphi}{\partial \overline{\boldsymbol{u}}}\frac{\partial \overline{\boldsymbol{u}}}{\partial \boldsymbol{u}}\right)^\top = \left(\frac{\partial \overline{\boldsymbol{u}}}{\partial \boldsymbol{u}}\right)^\top \overline{\boldsymbol{K}}\overline{\boldsymbol{u}} = \boldsymbol{T}^\top \overline{\boldsymbol{f}} \tag{14}$$

is defined as a derivative of the strain energy $\varphi = 0.5\,\overline{\boldsymbol{u}}^\top \overline{\boldsymbol{K}}\overline{\boldsymbol{u}}$ with respect to the global nodal displacements $\boldsymbol{u}$. The expression of the transformation matrix $\boldsymbol{T} = \frac{\partial \overline{\boldsymbol{u}}}{\partial \boldsymbol{u}}$ is not straightforward to obtain because the derivative of Eq. (13) involves a derivative of the rotation matrix. In [6], it is expressed as

$$\boldsymbol{T}^\top = \left(\frac{\partial \overline{\boldsymbol{u}}}{\partial \boldsymbol{u}}\right)^\top = \operatorname{diag}(\boldsymbol{R}) + \boldsymbol{V}\boldsymbol{Z}^\top, \tag{15}$$

where the $3N \times 3$ term $\boldsymbol{V}$, which is not explicitly named in [6], is given by

$$\boldsymbol{V} = -\operatorname{diag}(\boldsymbol{R})\boldsymbol{A}(\boldsymbol{Z}^\top\boldsymbol{A})^{-1} \Leftrightarrow \operatorname{diag}(\boldsymbol{R})\overline{\boldsymbol{G}}^\top\boldsymbol{R}^\top = \boldsymbol{G}^\top \tag{16}$$

and where $\overline{\boldsymbol{G}}$ and $\boldsymbol{G}$ are the local and global spin-fitter matrix, respectively, which are defined in the next section, and the nameless $3N \times 3$ term $\boldsymbol{Z}$ is

$$\boldsymbol{Z} = \operatorname{diag}(\boldsymbol{R}^\top)\operatorname{col}(\boldsymbol{S}(\boldsymbol{x}_{i\mathrm{o}})) = -\operatorname{diag}(\boldsymbol{R}^\top)\begin{bmatrix} -\operatorname{spin}(\boldsymbol{x}_{1\mathrm{o}}) \\ \vdots \\ -\operatorname{spin}(\boldsymbol{x}_{N\mathrm{o}}) \end{bmatrix} \Leftrightarrow -\operatorname{diag}(\boldsymbol{R}^\top)\boldsymbol{S} = \tag{17}$$

$$= -\operatorname{diag}(\boldsymbol{R}^\top)\boldsymbol{S}\boldsymbol{R}\boldsymbol{R}^\top = -\overline{\boldsymbol{S}}\boldsymbol{R}^\top, \tag{18}$$

where $\boldsymbol{x}_{i\mathrm{o}} = \boldsymbol{x}_i - \boldsymbol{x}_{\mathrm{o}}$ is a global coordinate of the node i with respect to the LCS origin, here node 1, in the current, i.e. deformed, configuration, the operator *col* forms a column $3N \times 3$ matrix, and $\overline{\boldsymbol{S}}$ and $\boldsymbol{S}$ are the local and global spin-lever matrix, respectively, defined in the next section.

The transformation matrix according to Crisfield and Moita seems to have a different form than the one with a projector matrix used by many other authors, including Felippa and Haugen. However, inserting Eq. (16) and Eq. (18) to Eq. (15) yields the transformation matrix in the following form

$$\boldsymbol{T}^\top = \operatorname{diag}(\boldsymbol{R})[\boldsymbol{I}_{3N} - \boldsymbol{A}(\overline{\boldsymbol{S}}^\top\boldsymbol{A})^{-1}\overline{\boldsymbol{S}}^\top] = \operatorname{diag}(\boldsymbol{R})(\boldsymbol{I}_{3N} - \overline{\boldsymbol{S}\boldsymbol{G}})^\top, \tag{19}$$

where $\boldsymbol{I}_{3N}$ is an $3N \times 3N$ identity matrix, the identity $\boldsymbol{R}^{-1}\boldsymbol{R} = \boldsymbol{I}$ was used, and the term $\boldsymbol{I}_{3N} - \overline{\boldsymbol{S}\boldsymbol{G}}$ represents the nonlinear projector matrix $\overline{\boldsymbol{P}}$.

The resulting internal force vector

$$\boldsymbol{f} = \boldsymbol{T}^\top \overline{\boldsymbol{f}} = [\mathrm{diag}(\boldsymbol{R}) + \boldsymbol{V}\boldsymbol{Z}^\top]\overline{\boldsymbol{K}}\overline{\boldsymbol{u}} \Leftrightarrow \mathrm{diag}(\boldsymbol{R})(\boldsymbol{I}_{3N} - \overline{\boldsymbol{S}\boldsymbol{G}})^\top \overline{\boldsymbol{K}}\overline{\boldsymbol{u}} = \mathrm{diag}(\boldsymbol{R})\overline{\boldsymbol{P}}^\top \overline{\boldsymbol{f}} \tag{20}$$

is equivalent to Felippa's formulation in [9]. The local internal force vector $\overline{\boldsymbol{f}}$ is first corrected in the LCS by the projector matrix and then rotated back to the GCS. Although Crisfield and Moita do not mention it, they use a projector matrix to express the internal force vector.

2.4 Tangent stiffness matrix

The consistent tangent stiffness matrix of an element

$$\boldsymbol{K} = \left(\frac{\partial^2 \varphi}{\partial \boldsymbol{u}^2}\right)^\top = \left(\frac{\partial \boldsymbol{f}}{\partial \boldsymbol{u}}\right)^\top = \boldsymbol{T}^\top \overline{\boldsymbol{K}}\boldsymbol{T} + \left.\frac{\partial(\boldsymbol{T}^\top \overline{\boldsymbol{f}})}{\partial \boldsymbol{u}^\top}\right|_{\overline{\boldsymbol{f}}=\text{const.}} = \boldsymbol{K}_\mathrm{m} + \boldsymbol{K}_\mathrm{g} \tag{21}$$

is defined as a derivative of the internal force vector with respect to the global nodal displacements. The derivative of Eq. (20) yields two parts, the material tangent stiffness matrix $\boldsymbol{K}_\mathrm{m}$ and the geometric tangent stiffness matrix $\boldsymbol{K}_\mathrm{g}$, whose derivation is mathematically involved.

The resulting tangent stiffness matrix according to Crisfield and Moita is

$$\boldsymbol{K} = \boldsymbol{T}^\top \overline{\boldsymbol{K}}\boldsymbol{T} - \mathrm{col}(\boldsymbol{S}(\overline{\boldsymbol{f}}_\mathrm{r}))\boldsymbol{V}^\top + \boldsymbol{V}\,\mathrm{row}(\boldsymbol{S}(\overline{\boldsymbol{f}}_r)) + \boldsymbol{V}\,\mathrm{sym}\sum_{i=1}^{N}\left[\boldsymbol{S}(\boldsymbol{x}_{\mathrm{io}})\boldsymbol{S}(\overline{\boldsymbol{f}}_{r,i})\right]\boldsymbol{V}^\top, \tag{22}$$

where the last term is artificially symmetrized via the *sym* operator and where

$$\begin{aligned} -\mathrm{col}(\boldsymbol{S}(\overline{\boldsymbol{f}}_\mathrm{r})) = [\mathrm{row}(\boldsymbol{S}(\overline{\boldsymbol{f}}_r))]^\top \Leftrightarrow \begin{bmatrix} -\mathrm{spin}(\overline{\boldsymbol{f}}_{\mathrm{r},1}) \\ \cdots \\ -\mathrm{spin}(\overline{\boldsymbol{f}}_{\mathrm{r},i}) \\ \cdots \\ -\mathrm{spin}(\overline{\boldsymbol{f}}_{\mathrm{r,N}}) \end{bmatrix} &= \begin{bmatrix} -\mathrm{spin}(\boldsymbol{R}\overline{\boldsymbol{f}}_1) \\ \cdots \\ -\mathrm{spin}(\boldsymbol{R}\overline{\boldsymbol{f}}_i) \\ \cdots \\ -\mathrm{spin}(\boldsymbol{R}\overline{\boldsymbol{f}}_\mathrm{N}) \end{bmatrix} \\ = -\mathrm{diag}(\boldsymbol{R}) \begin{bmatrix} \mathrm{spin}(\overline{\boldsymbol{f}}_1) \\ \cdots \\ \mathrm{spin}(\overline{\boldsymbol{f}}_i) \\ \cdots \\ \mathrm{spin}(\overline{\boldsymbol{f}}_\mathrm{N}) \end{bmatrix} \boldsymbol{R}^\top &= -\mathrm{diag}(\boldsymbol{R})\overline{\boldsymbol{F}}_\mathrm{C}\boldsymbol{R}^\top, \end{aligned} \tag{23}$$

where the identity $\mathrm{spin}(\boldsymbol{R}\overline{\boldsymbol{f}}_i) = \boldsymbol{R}\,\mathrm{spin}(\overline{\boldsymbol{f}}_i)\boldsymbol{R}^\top$ is applied.

For comparison purposes, inserting Eq. (16), Eq. (20) and Eq. (23) to Eq. (22) and utilizing $\boldsymbol{R}^\top \boldsymbol{R} = \boldsymbol{I}$ yields Crisfield's tangent stiffness matrix in Felippa's notation

$$\begin{aligned}\boldsymbol{K} = &\operatorname{diag}(\boldsymbol{R})\,\overline{\boldsymbol{P}}^\top \overline{\boldsymbol{K}\boldsymbol{P}}\operatorname{diag}(\boldsymbol{R}^\top) - \operatorname{diag}(\boldsymbol{R})\,\overline{\boldsymbol{F}}_{\mathrm{C}}\,\overline{\boldsymbol{G}}\operatorname{diag}(\boldsymbol{R}^\top) \\ &- \operatorname{diag}(\boldsymbol{R})\,\overline{\boldsymbol{G}}^\top\,\overline{\boldsymbol{F}}_{\mathrm{C}}^\top\operatorname{diag}(\boldsymbol{R}^\top) + \operatorname{diag}(\boldsymbol{R})\,\overline{\boldsymbol{G}}^\top\operatorname{sym}(\overline{\boldsymbol{S}}^\top\overline{\boldsymbol{F}}_{\mathrm{C}})\overline{\boldsymbol{G}}\operatorname{diag}(\boldsymbol{R}^\top).\end{aligned} \tag{24}$$

Since the consistent tangent stiffness matrix is a Hessian of the strain energy, it should result in a symmetric matrix. In Eq. (22), the first term is symmetric, the third is the transpose of the second, preserving the symmetry, and the fourth term is artificially symmetrized. Crisfield and Moita claim that the non-symmetric part $\sum_{i=1}^{N} \boldsymbol{x}_{i\mathrm{o}} \times \overline{\boldsymbol{f}}_{r,i}$ of the fourth term vanishes at equilibrium and therefore can be neglected [6]. However, as reported in [8], it is a misconception stemming from the fact that for the cross-product representing the element global moment equilibrium, the rotated local internal forces $\overline{\boldsymbol{f}}_{\mathrm{r}} = \operatorname{diag}(\boldsymbol{R})\overline{\boldsymbol{f}}$ were considered instead of the global internal forces $\boldsymbol{f} = [\operatorname{diag}(\boldsymbol{R}) + \boldsymbol{V}\boldsymbol{Z}^\top]\overline{\boldsymbol{f}}$ which additionally include the projector. Since the variation of $\boldsymbol{V}$ was ignored, the resulting Crisfield's tangent stiffness matrix is inconsistent, missing three additional terms as shown in [8], and had to be artificially symmetrized. Fortunately, this misconception does not influence the resulting displacements, since they are prescribed by the correct internal forces. It only slows down the convergence rate of the incremental iterative procedure.

3 Felippa's co-rotational formulation

Felippa's CR formulation was developed by Felippa and Haugen and is well explained in their seminal work [9]. Although the authors focus on structural FEs, i.e., shells and beams, their principles are also valid for solid FEs, which do not possess additional rotational DOFs.

3.1 Rotation matrix

The origin of the LCS is placed at the element centroid. In the case of beams and shells, the orientation of the LCS, expressed by the rotation matrix, can be determined via the side-alignment approach or a best-fit procedure. However, the determination of the rotation matrix for 3D solid FEs is not specified in their work.

3.2 Local deformational displacements

In [9], a general, initially rotated LCS is assumed. This is particularly useful in the case of beams and shells, where the LCS is often constructed using the side-alignment approach, where one coordinate axis goes through two algorithmically selected element nodes. However, for solid FEs, the initial LCS can be assumed parallel with the

GCS, which turns the initial rotation matrix to identity. Felippa's local deformational displacement vector is then simplified to the following form

$$\begin{aligned}
\overline{\boldsymbol{u}} &= \operatorname{diag}(\boldsymbol{R}^\top)\boldsymbol{u}_\mathrm{d} \\
&= \operatorname{diag}(\boldsymbol{R}^\top)\left[\boldsymbol{u} - \boldsymbol{u}_\mathrm{o} - \left(\operatorname{diag}(\boldsymbol{R}) - \boldsymbol{I}_{3N}\right)\left(\boldsymbol{x}_0 - \boldsymbol{x}_{\mathrm{o},0}\right)\right] \\
&= \operatorname{diag}(\boldsymbol{R}^\top)\left[\boldsymbol{u} - \boldsymbol{u}_\mathrm{o} - \operatorname{diag}(\boldsymbol{R})(\boldsymbol{x}_0 - \boldsymbol{x}_{\mathrm{o},0}) + \boldsymbol{x}_0 - \boldsymbol{x}_{\mathrm{o},0}\right] \\
&= \operatorname{diag}(\boldsymbol{R}^\top)\left(\boldsymbol{u} - \boldsymbol{u}_\mathrm{o} + \boldsymbol{x}_0 - \boldsymbol{x}_{\mathrm{o},0}\right) - \operatorname{diag}(\boldsymbol{R}^\top)\operatorname{diag}(\boldsymbol{R})(\boldsymbol{x}_0 - \boldsymbol{x}_{\mathrm{o},0}) \\
&= \operatorname{diag}(\boldsymbol{R}^\top)\left(\boldsymbol{u} + \boldsymbol{x}_0 - \boldsymbol{u}_\mathrm{o} - \boldsymbol{x}_{\mathrm{o},0}\right) - \overline{\boldsymbol{x}}_0 \\
&\equiv \operatorname{diag}(\boldsymbol{R}^\top)\boldsymbol{x} - \overline{\boldsymbol{x}}_0,
\end{aligned} \tag{25}$$

where $\boldsymbol{u}_\mathrm{d}$ is the deformational part of the global displacement vector $\boldsymbol{u}$ measured in the GCS, $\boldsymbol{u}_\mathrm{o}$ represents the rigid body translation of the element LCS and the term $\left(\operatorname{diag}(\boldsymbol{R}) - \boldsymbol{I}_{3N}\right)\left(\boldsymbol{x}_0 - \boldsymbol{x}_{\mathrm{o},0}\right)$ represents the rigid body rotation of the element LCS. The resulting expression of the local deformational displacement vector is identical to Crisfield's formulation, see Eq. (12) . Again, the rigid body translations $\boldsymbol{u}_\mathrm{o}$ and $\boldsymbol{x}_{\mathrm{o},0}$ of the element LCS origin do not influence the internal force computation and therefore can be omitted.

3.3 Internal force

The internal force vector is defined following Eq. (14) as a transformed local internal force vector. In [9], the transformation matrix is defined as follows

$$\boldsymbol{T}^\top = \left(\frac{\partial \overline{\boldsymbol{u}}}{\partial \boldsymbol{u}}\right)^\top = \operatorname{diag}(\boldsymbol{R})\overline{\boldsymbol{P}}^\top\overline{\boldsymbol{H}}^\top, \tag{26}$$

where the matrix $\overline{\boldsymbol{H}}$ assigns identity matrices to the translational DOFs and the Jacobian derivatives of the rotational axial vectors with respect to the spin axial vectors to the rotational DOFs. Therefore, in the case of solid FEs, this matrix has no effect and is omitted.

The resulting internal force vector is

$$\boldsymbol{f} = \boldsymbol{T}^\top\overline{\boldsymbol{f}} = \operatorname{diag}(\boldsymbol{R})\overline{\boldsymbol{P}}^\top\overline{\boldsymbol{f}} = \operatorname{diag}(\boldsymbol{R})(\boldsymbol{I}_{3N} - \overline{\boldsymbol{S}\boldsymbol{G}})^\top\overline{\boldsymbol{f}}. \tag{27}$$

The local *spin-lever* or *moment-arm* matrix has dimensions $3N \times 3$ and is defined as

$$\begin{aligned}
\overline{\boldsymbol{S}} &= \begin{bmatrix}\operatorname{spin}(\overline{\boldsymbol{x}}_1) & \dots & \operatorname{spin}(\overline{\boldsymbol{x}}_N)\end{bmatrix}^\top = \begin{bmatrix}-\operatorname{spin}(\overline{\boldsymbol{x}}_1) \\ \vdots \\ -\operatorname{spin}(\overline{\boldsymbol{x}}_N)\end{bmatrix} = \operatorname{diag}(\boldsymbol{R}^\top)\begin{bmatrix}-\operatorname{spin}(\boldsymbol{x}_{1\mathrm{o}}) \\ \vdots \\ -\operatorname{spin}(\boldsymbol{x}_{N\mathrm{o}})\end{bmatrix}\boldsymbol{R} \\
&= \operatorname{diag}(\boldsymbol{R}^\top)\boldsymbol{S}\boldsymbol{R} \Leftrightarrow -\boldsymbol{Z}\boldsymbol{R},
\end{aligned} \tag{28}$$

where the *spin* operator is defined in Eq. (9), $\overline{\boldsymbol{x}}_i = \boldsymbol{R}^\top\boldsymbol{x}_{i\mathrm{o}} = \boldsymbol{R}^\top(\boldsymbol{x}_i - \boldsymbol{x}_\mathrm{o})$ is the local nodal position of the node i in the current configuration, $\boldsymbol{S}$ is the global spin-lever matrix and $\boldsymbol{Z}$ is mentioned here to define the link to Crisfield's formulation.

The local *spin-fitter* matrix, introduced by Haugen in [10], links variations in the element spin (instantaneous rotations) at the centroid of the deformed element in response to variations in the local nodal displacements $\delta\overline{\boldsymbol{\omega}} \coloneqq \overline{\boldsymbol{G}}\,\delta\overline{\boldsymbol{u}}$. Unlike $\overline{\boldsymbol{S}}$, the $\overline{\boldsymbol{G}}$ matrix depends not only on element geometry, but also on the method of the LCS construction. Probably, for this reason, its derived form is rarely presented in the literature.

The local *spin-fitter* matrix for 3D solid FEs has dimensions $3 \times 3N$ and, for the LCS constructed by the polar decomposition method, it can be computed, utilizing the matrix $\boldsymbol{A}$ defined in Eq. (7), as follows

$$\begin{aligned}\overline{\boldsymbol{G}} &= \left[\frac{\partial\overline{\boldsymbol{\omega}}}{\partial\overline{\boldsymbol{u}}_1} \quad \cdots \quad \frac{\partial\overline{\boldsymbol{\omega}}}{\partial\overline{\boldsymbol{u}}_\mathrm{N}}\right] = (\boldsymbol{A}^\top\overline{\boldsymbol{S}})^{-1}\boldsymbol{A}^\top \Leftrightarrow -\boldsymbol{R}^\top(\boldsymbol{A}^\top\boldsymbol{Z})^{-1}\boldsymbol{A}^\top \\ &= \boldsymbol{R}^\top\left[-(\boldsymbol{A}^\top\boldsymbol{Z})^{-1}\boldsymbol{A}^\top\,\mathrm{diag}(\boldsymbol{R}^\top)\right]\mathrm{diag}(\boldsymbol{R}) = \boldsymbol{R}^\top\boldsymbol{G}\,\mathrm{diag}(\boldsymbol{R}),\end{aligned} \tag{29}$$

where the last expression in Eq. (28) is utilized, $\boldsymbol{G}$ is the global spin-fitter matrix, and $\boldsymbol{Z}$ is mentioned here to define the link to Crisfield's formulation.

The projector matrix $\overline{\boldsymbol{P}} = \boldsymbol{I}_{3N} - \overline{\boldsymbol{S}}\overline{\boldsymbol{G}}$ in Eq. (27) ensures that the local internal forces at the element nodes are in a moment balance. The term $\overline{\boldsymbol{S}}^\top\overline{\boldsymbol{f}} = \sum_{i=1}^{N}\mathrm{spin}(\overline{\boldsymbol{x}}_i)\overline{\boldsymbol{f}}_i = \sum_{i=1}^{N}\overline{\boldsymbol{x}}_i \times \overline{\boldsymbol{f}}_i = \overline{\boldsymbol{m}}_\mathrm{u}$ represents the local unbalanced moment. The spin fitter matrix then turns it into the local unbalance force $\overline{\boldsymbol{f}}_\mathrm{u} = \overline{\boldsymbol{G}}^\top\overline{\boldsymbol{S}}^\top\overline{\boldsymbol{f}} = \overline{\boldsymbol{G}}^\top\overline{\boldsymbol{m}}_\mathrm{u}$ which is projected out of the local internal force $\overline{\boldsymbol{f}}$. The projected local force $\overline{\boldsymbol{f}}_\mathrm{p}$ does not produce an unbalanced moment

$$\overline{\boldsymbol{S}}^\top\overline{\boldsymbol{f}}_\mathrm{p} = \overline{\boldsymbol{S}}^\top(\boldsymbol{I}_{3\mathrm{N}} - \overline{\boldsymbol{G}}^\top\overline{\boldsymbol{S}}^\top)\overline{\boldsymbol{f}} = \boldsymbol{0}, \tag{30}$$

because the bi-orthogonality condition $\overline{\boldsymbol{G}}\overline{\boldsymbol{S}} = \overline{\boldsymbol{S}}^\top\overline{\boldsymbol{G}}^\top = \boldsymbol{I}$, established in [15], applies. Therefore, $\overline{\boldsymbol{P}}$ has its idempotent projector property

$$\overline{\boldsymbol{P}}^2 = \boldsymbol{I}_{3N} - 2\overline{\boldsymbol{S}}\overline{\boldsymbol{G}} + \overline{\boldsymbol{S}}\overline{\boldsymbol{G}}\overline{\boldsymbol{S}}\overline{\boldsymbol{G}} = \boldsymbol{I}_{3N} - \overline{\boldsymbol{S}}\overline{\boldsymbol{G}} = \overline{\boldsymbol{P}}. \tag{31}$$

The origin of the local unbalanced moment and the need for the projector result from the *imperfect* computation of the element rotation matrix. Since most of the solid FEs allow different rotations at their various points, the rotation matrix calculated in the element centroid cannot always substitute the exact *mean* element rotation [7]. It is just a good approximation. The only exceptions are the triangular and tetrahedral FEs that have a constant deformation gradient. Their rotation matrix, computed in element centroid, represents exactly the rigid body rotation of the whole FE, and the projector matrix has no use there.

3.4 Tangent stiffness

The consistent tangent stiffness matrix of a solid element

$$\boldsymbol{K} = \left(\frac{\partial^2\varphi}{\partial\boldsymbol{u}^2}\right)^\top = \left(\frac{\partial\boldsymbol{f}}{\partial\boldsymbol{u}}\right)^\top = \boldsymbol{K}_\mathrm{m} + \boldsymbol{K}_\mathrm{gr} + \boldsymbol{K}_\mathrm{gp} \tag{32}$$

is defined as a derivative of the internal force vector with respect to the global nodal displacements. The derivative of the internal force vector $\boldsymbol{f} = \mathrm{diag}(\boldsymbol{R})\overline{\boldsymbol{P}}^{\top}\overline{\boldsymbol{f}}$ from Eq. (27) yields the following three parts. The material stiffness matrix $\boldsymbol{K}_{\mathrm{m}}$ is the result of the variation of the local internal force $\overline{\boldsymbol{f}}$ and is given by a congruent transformation of the local stiffness matrix $\overline{\boldsymbol{K}}$ to the GCS. The rotational geometric stiffness matrix $\boldsymbol{K}_{\mathrm{gr}}$ results from the variation of the element rotation matrix $\mathrm{diag}(\boldsymbol{R})$ and represents the gradient of the internal force vector with respect to the rigid rotation of the element. The equilibrium projection geometric stiffness matrix $\boldsymbol{K}_{\mathrm{gp}}$ results from the variation of the projector $\overline{\boldsymbol{P}}$ and represents the variation of the projection of the local internal force as the element geometry changes.

The resulting tangent stiffness matrix for a 3D solid finite element according to Felippa and Haugen is

$$\begin{aligned}\boldsymbol{K} &= \mathrm{diag}(\boldsymbol{R})\overline{\boldsymbol{P}}^{\top}\frac{\partial\overline{\boldsymbol{f}}}{\partial\boldsymbol{u}^{\top}} + \left.\frac{\partial(\mathrm{diag}(\boldsymbol{R})\overline{\boldsymbol{f}}_{\mathrm{p}})}{\partial\boldsymbol{u}^{\top}}\right|_{\overline{\boldsymbol{f}}_{\mathrm{p}}=\text{const.}} + \mathrm{diag}(\boldsymbol{R})\left.\frac{\partial(\overline{\boldsymbol{P}}^{\top}\overline{\boldsymbol{f}})}{\partial\boldsymbol{u}^{\top}}\right|_{\overline{\boldsymbol{f}}=\text{const.}} \\ &= \mathrm{diag}(\boldsymbol{R})\overline{\boldsymbol{P}}^{\top}\overline{\boldsymbol{K}\boldsymbol{P}}\mathrm{diag}(\boldsymbol{R}^{\top}) - \mathrm{diag}(\boldsymbol{R})\overline{\boldsymbol{F}\boldsymbol{G}}\mathrm{diag}(\boldsymbol{R}^{\top}) - \mathrm{diag}(\boldsymbol{R})\overline{\boldsymbol{G}}^{\top}\overline{\boldsymbol{F}}^{\top}\overline{\boldsymbol{P}}\mathrm{diag}(\boldsymbol{R}^{\top}),\end{aligned} \tag{33}$$

where $\overline{\boldsymbol{f}}_{\mathrm{p}} = \overline{\boldsymbol{P}}^{\top}\overline{\boldsymbol{f}}$ is the projected local internal force vector and whose nodal components are transformed into the skew-symmetric matrices that are stacked to a $3N \times 3$ matrix

$$\overline{\boldsymbol{F}} = \begin{bmatrix}\mathrm{spin}(\overline{\boldsymbol{f}}_{\mathrm{p}1}) \\ \vdots \\ \mathrm{spin}(\overline{\boldsymbol{f}}_{\mathrm{p}N})\end{bmatrix}. \tag{34}$$

In the case of elements with rotational DOFs, the term $\overline{\boldsymbol{F}}$ in $\boldsymbol{K}_{\mathrm{gr}}$ is not the same as in $\boldsymbol{K}_{\mathrm{gp}}$, and two additional geometric stiffness terms $\boldsymbol{K}_{\mathrm{gm}}$ and $\Delta\boldsymbol{K}_{\mathrm{gp}}$ appear in the consistent tangent stiffness matrix, see e.g. [9] for details.

The tangent stiffness matrix is symmetric without neglecting any terms. Comparing Felippa's tangent stiffness matrix in Eq. (33) to Crisfield's one in Eq. (24), one can clearly see that the first three terms look similar. However, $\overline{\boldsymbol{F}}_{\mathrm{C}}$ is built from only the local internal forces, whereas $\overline{\boldsymbol{F}}$ is built from the projected local internal forces.

4 Conclusions

In this study, two established (CR) formulations, Crisfield's and Felippa's, have been systematically rewritten using a unified notation, enabling a direct and transparent comparison. Although Crisfield's formulation does not explicitly mention projectors, it implicitly employs them. The key contribution of this paper is an explicit formulation of Crisfield's matrix $\boldsymbol{A}$ and Felippa's spin-fitter matrix $\boldsymbol{G}$ in a ready-to-implement matrix

form for 3D solid FEs, whose rotation matrix is computed by the polar decomposition of the deformation gradient.

The mathematical expressions throughout the paper have been reformulated to enhance clarity and interpretability. Despite initial differences in the expressions for deformational displacement vectors, it has been demonstrated that they are mathematically equivalent. The internal force vectors derived from both formulations are also shown to be identical. They both rely on the same projection operator, ensuring equilibrium not only in forces but also in moments. As a result, both formulations yield the same displacement fields for given loads and boundary conditions.

However, the formulations differ in their computation of the rotation matrix, reflecting their original application focus, with Felippa targeting beams and shells, and Crisfield accommodating also 3D solids. Furthermore, the tangent stiffness matrices are not equivalent. Crisfield, like many other authors, omits some higher-order terms arising during the derivation, which affects the speed of the incremental-iterative solution procedure but not its accuracy, which is completely defined by the internal force vector. Consequently, Felippa's consistent tangent stiffness matrix is expected to reach the convergent solution with fewer NR iterations.

Based on these findings, the authors are developing a new CR formulation for 3D solid FEs that synthesizes the strengths of both Crisfield's and Felippa's approaches. The algorithm and its numerical performance will be presented in a forthcoming journal publication.

Acknowledgements

The presented work was supported by: the Specific Reasearch (SP2025/048); EU funds through the Operational Programme Johannes Amos Comenius (CZ.02.01.01/00/23_021/0008759); the science and research support in the Moravian-Silesian region (RRC/12/2022).

References

[1] WEMPNER, G. Finite Elements, Finite Rotations and Small Strains of Flexible Shells. *International Journal of Solids and Structures*. 1969, vol. 5, no. 2, pp. 117–153. Available from DOI: 10.1016/0020-7683(69)90025-0.

[2] BELYTSCHKO, T.; HSIEH, B. J. Non-Linear Transient Finite Element Analysis with Convected Co-Ordinates. *International Journal for Numerical Methods in Engineering*. 1973, vol. 7, no. 3, pp. 255–271. Available from DOI: 10.1002/nme.1620070304.

[3] RANKIN, C. C.; BROGAN, F. A. An Element Independent Corotational Procedure for the Treatment of Large Rotations. *Journal of Pressure Vessel Technology*. 1986, vol. 108, no. 2, pp. 165–174. Available from DOI: 10.1115/1.3264765.

[4] CRISFIELD, M.; MOITA, G. A Unified Co-Rotational Framework for Solids, Shells and Beams. *International Journal of Solids and Structures*. 1996, vol. 33, no. 20, pp. 2969–2992. Available from DOI: https://doi.org/10.1016/0020-7683(95)00252-9.

[5] MOITA, G. F. *Non-Linear Finite Element Analysis of Continua with Emphasis on Hyperelasticity*. 1994. Ph.D. thesis. Imperial College London.

[6] MOITA, G.; CRISFIELD, M. A Finite Element Formulation for 3-D Continua Using the Co-Rotational Technique. *International Journal for Numerical Methods in Engineering*. 1996, vol. 39, no. 22, pp. 3775–3792. Available from DOI: 10.1002/(SICI)1097-0207(19961130)39:22<3775::AID-NME23>3.0.CO;2-W.

[7] KAN, Z.; DONG, K.; CHEN, B.; PENG, H.; SONG, X. The Direct Force Correction Based Framework for General Co-Rotational Analysis. *Computer Methods in Applied Mechanics and Engineering*. 2021, vol. 385, p. 114018. Available from DOI: 10.1016/j.cma.2021.114018.

[8] LESIV, H.; IZZUDDIN, B. Consistency and Misconceptions in Co-Rotational 3D Continuum Finite Elements: A Zero-Macrospin Approach. *International Journal of Solids and Structures*. 2023, vol. 281, p. 112445. Available from DOI: 10.1016/j.ijsolstr.2023.112445.

[9] FELIPPA, C.; HAUGEN, B. A Unified Formulation of Small-Strain Corotational Finite Elements: I. Theory. *Computer Methods in Applied Mechanics and Engineering*. 2005, vol. 194, no. 21, pp. 2285–2335. Available from DOI: https://doi.org/10.1016/j.cma.2004.07.035.

[10] HAUGEN, B. *Buckling and Stability Problems for Thin Shell Structures Using High Performance Finite Elements*. 1994. Ph.D. thesis. University of Colorado.

[11] PALENIK, R.; MOLCAN, M.; PORUBA, Z. Comparison of Co-Rotational and Nonlinear Finite Element Simulations with Geometric Nonlinearities. In: *Engineering Mechanics 2022: 27/28th international conference*. 2022.

[12] JETTEUR, P.; CESCOTTO, S. A Mixed Finite Element for the Analysis of Large Inelastic Strains. *International Journal for Numerical Methods in Engineering*. 1991, vol. 31, no. 2, pp. 229–239. Available from DOI: 10.1002/nme.1620310203.

[13] CRISFIELD, M. A.; MOITA, G. F. A Co-Rotational Formulation for 2-D Continua Including Incompatible Modes. *International Journal for Numerical Methods in Engineering*. 1996, vol. 39, no. 15, pp. 2619–2633. Available from DOI: 10.1002/(SICI)1097-0207(19960815)39:15<2619::AID-NME969>3.0.CO;2-N.

[14] RANKIN, C. Application of Linear Finite Elements to Finite Strain Using Corotation. In: 2006, vol. 3. Available from DOI: 10.2514/6.2006-1751.

[15] RANKIN, C.; NOUR-OMID, B. The Use of Projectors to Improve Finite Element Performance. In: NOOR, A. K.; DWOYER, D. L. (eds.). *Computational Structural Mechanics & Fluid Dynamics*. Oxford: Pergamon, 1988, pp. 257–267. Available from DOI: https://doi.org/10.1016/B978-0-08-037197-9.50028-0.